



Volume XXIV 2021

ISSUE no.1

MBNA Publishing House Constanta 2021



## Scientific Bulletin of Naval Academy

SBNA PAPER • OPEN ACCESS

### The potential air flow through diver's breathing apparatus

To cite this article: T. STANCIU, A. AGAPE, N. CHIRIPUCI, P. FLESER and C. MUNTEANU, Scientific Bulletin of Naval Academy, Vol. XXIV 2021, pg.41-47.

Submitted: 03.03.2021

Revised: 15.06.2021

Accepted: 22.07.2021

Available online at [www.anmb.ro](http://www.anmb.ro)

ISSN: 2392-8956; ISSN-L: 1454-864X

doi: 10.21279/1454-864X-21-I1-004

SBNA© 2021. This work is licensed under the CC BY-NC-SA 4.0 License

# The potential air flow through diver's breathing apparatus

T Stanciu, A Agape, N Chiripuci, P Fleser, C Munteanu

Diving Center, 19 "1 May." Blvd, Constantza, Romania

**Abstract:** The gas admission through the divers' breathing apparatus is done with a critical flow. The gas storage pressure is reduced to the value of the external pressure  $p_e$ . The paper approaches the gas-dynamic phenomena that occur when the gas flows through the second stage regulator, respectively: the variable restrictor A (between the seat and the cylindrical piston) and the fixed restrictor B (the orifice of cylindrical piston). The two main pressure restrictors can be considered Laval nozzles. Mathematical modeling of airflow through restrictors was done following the notions of the theory of potential gas flow through tubes and nozzles. The air flow was calculated numerically and by CFD simulation and was experimentally verified at a professional stand for the second stage.

## 1. Introduction

The diving specialists are constantly concerned with the safety of divers and improving their comfort in immersing, whether their activity is commercial or military. The gas becomes more dense with increasing depth (pressure), causing increased respiratory resistance. The anatomically dead volume also increases. Knowing the respiratory flow of gas in various situations is necessary to control the physical and physiological phenomena involved, to choose a breathing apparatus that reduces resistance to inspiration and expiration and thus the user's effort.

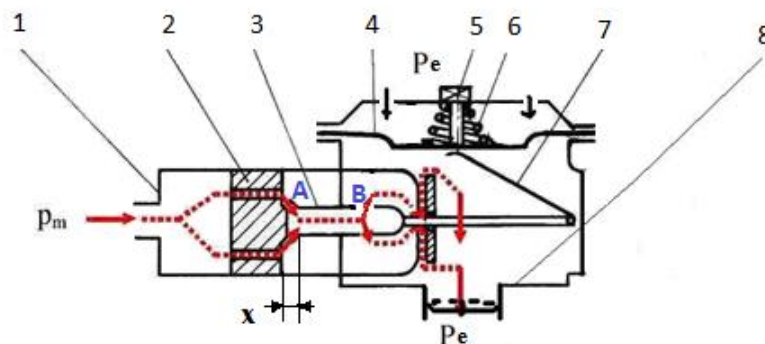


Figure 1 [1]

### Unbalanced second stage regulator with downstream admission

- 1- casing, 2 - sealing seat, 3 -poppet tube, 4 - membrane, 5 -adjusting screw, 6 - spring, 7 - lever, 8 -exhale valve

The storage air pressure in the diver's cylinder is reduced, by the first stage, to an average pressure  $p_m$ . The gas passes through the medium pressure hose and reaches the second pressure regulator. The second stage regulator, showed in Figure 1, is unbalanced with downstream admission. Respiratory air is admitted in the second stage at the average pressure higher by 8.5 , above the outlet pressure  $p_e$ . The opening of the reducer is triggered by the inhalation of air at  $5\text{-}6 \cdot 10^2 [Pa]$  of vacuum, which moves the membrane (4), the membrane that pushes the lever (7). The lever actuates the poppet tube (3) by moving it again between the poppet tube and the seat (2). In the point **A** is the first restrictor composed of the poppet tube (3) and its sealing seat (2) with variable flow area. The second restrictor **B** is the orifice in the poppet tube wall with constant flow area. Only the two series-mounted pressure restrictors **A** and **B** were considered (see Fig. 1).

## 2. Mathematical modeling of potential air flow through the restrictors of second stage

The paper approaches the gas-dynamic phenomena that occur when the gas flows through the second stage reducer, respectively: the variable restrictor **A** (between the seat and the poppet tube) and the fixed restrictor **B** (the orifice of cylindrical piston). Mathematical modeling of potential air flow through the restrictors of breathing apparatus was made following the notions of the theory of the potential flow of gases through tubes and nozzles. [1] The two restrictors can be considered Laval nozzles.

For the study we established a simplified model of a classic downstream flow regulator, in which we took into account 2 versions. In the 1<sup>st</sup> version the fixed restrictor **B** is cylindrical and in the 2<sup>nd</sup> version the fixed restrictor **B** is a conical nozzle. The variable area of the restrictor **A** is critical, the flow is also critical. The variable restrictor **A** is a convergent-divergent nozzle (Laval). The flow is stationary and turbulent. When the gas passes through the minimum section, it reaches critical speed and the pressure drops. Due to this difference between the critical pressure  $p_c$  and the outlet pressure  $p_e$ , an expanding gas jet is formed, which passes through a shock wave system. The minimum section in which the critical speed is reached is the critical section  $A_c$ , all the parameters involved are critical. [2]

Respiratory gas is air. The supply parameters of the second stage regulator have average values, respectively:

$p_m = 9.5 \cdot 10^5 [Pa]$  – medium hose pressure

$p_b [kg/m^3] = 150 \cdot 10^5 [Pa]$  – cylinder pressure

$\rho_m [kg/m^3]$  – medium density of the air in the hose

$k = 1.4$  - adiabatic index of air

$T_b = 293K$  - cylinder temperature

For an adiabatic and isentropic evolution, we determined the air density at the storage pressure:

$$\rho_b = \frac{p_b}{RT_b} = \frac{150 \cdot 10^5}{287 \cdot 293} = 178.37 [kg/m^3] \quad (1)$$

The Reynolds number at the **A** variable restrictor is:

$$Re = \frac{\rho_b w d}{\eta} \quad (2)$$

$w [m/s] = 290m/s$  - air velocity in the critical area [1]

$d [m] = 0.005m$  – inner diameter of the cylinder

$R = 287 [\frac{J}{kgK}]$  - air constant

$\eta = 1.745 \cdot 10^{-10} [Ns/m^2]$  - dynamic viscosity,  $\mu$ , at 20°C [3]

$Re = 10^{10} \rightarrow$  the flow is turbulent at restrictor.

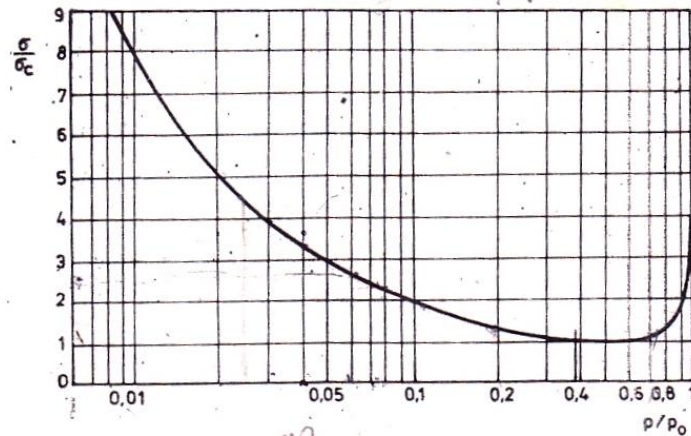


**Figure 2 Diagram of pressures distribution [2]**

**The 1<sup>st</sup> version** with the cylindrical orifice to the thin-walled piston, the **B** fixed restrictor. Knowing  $A_f$ , the area of the admission orifice, from the diagram (Fig. 2), results the area of the critical section,  $A_c = 10.9 \cdot 10^{-6} [m^2]$ , for the restrictor **A**. Piston displacement, for  $\Delta p = 5 \cdot 10^2 [Pa]$ , opening differential pressure is  $x = 0.0007 [m]$  at the restrictor **A**, for the critical pressure. [1] In the critical section, the maximum mass flow  $\dot{m}_c [kg/s]$  is reached, according to the continuity equation for a current tube [4].

$$\dot{m}_c = \rho_c A_c c \quad (3)$$

$\dot{m}_c$ , critical maximum flow

$\rho_c$ , density in critical conditions, respectively  $\rho_c, p_c, T_c$ .

$A_c$ , restrictor's area in critical conditions, respectively  $\rho_c, p_c, T_c$ .

$c$ , sound's speed in critical conditions, respectively  $\rho_c, p_c, T_c$ .

In a previous paper the maximum airflow was calculated for an ideal thermodynamic process, in which the flow rate coefficients through the two restrictors are:

$$\alpha_{1t} = \alpha_{2t} = 1$$

The calculated theoretical mass flow remains constant for this geometry and it is: [5]

$$\dot{m}_{t1} = \dot{m}_{t2} = \left( \frac{2}{k+1} \right)^{\frac{1}{2} \frac{(k+1)}{(k-1)}} \cdot \sqrt{k} \cdot A_c \cdot \frac{p_m}{\sqrt{RT_m}} = 0.025 [kg/s] \quad (4)$$

For the 1<sup>st</sup> version, with the cylindrical orifice at the **B** fixed restrictor, the real flow rate coefficient is:  $\alpha_{1r} = 0.7$ .

Real flow for the 1<sup>st</sup> version at  $\Delta p = 5 \cdot 10^2 [Pa]$  is:

$$\dot{m}_1 = \dot{m}_2 = \alpha_1 \dot{m}_{t1} = 0.7 \cdot 0.025 = 0.0175 [kg/s] \quad (5)$$

Piston displacement for  $\Delta p = 6 \cdot 10^2 [Pa]$  opening differential pressure is  $x = 0.0008 [m]$  at the restrictor **A**, for the critical pressure. Critical area is  $A_c = 12.6 \cdot 10^{-6} [m^2]$ .

Real flow for the 1<sup>st</sup> version at  $\Delta p = 6 \cdot 10^2 [Pa]$  is:

$$\dot{m}_1 = \dot{m}_2 = \alpha_{2r} \dot{m}_{t1} = 0.8 \cdot 0.025 = 0.020 [kg/s] \quad (6)$$

**The 2<sup>nd</sup> version** with a conical orifice at the **B** fixed restrictor

At  $\Delta p = 5 \cdot 10^2 [Pa]$ , the theoretical mass flow is the one calculated for the 1<sup>st</sup> version, the geometry of the restrictor **A** is unchanged, as well as the flow conditions.

$$\dot{m}_{t1} = \dot{m}_{t2} = 0.025 [kg/s]$$

The flow rate coefficient changes at the fixed restrictor **B**, for  $d = 6 \cdot 10^{-3} [m]$ :  $\alpha_{2r} = 0.8$

The real mass flow for the 2<sup>nd</sup> version at  $\Delta p = 5 \cdot 10^2 [Pa]$  is:

$$\dot{m}_1 = \dot{m}_2 = \alpha_{2r} \dot{m}_{t1} = 0.8 \cdot 0.025 = 0.020 [kg/s] \quad (7)$$

For  $\Delta p = 6 \cdot 10^2 [Pa]$ , the critical area is  $A_c = 12.6 \cdot 10^{-6} [m^2]$ , resulting displacement  $x = 0.0008 [m]$   
 The theoretical mass flow is:

$$\dot{m}_{t1} = \dot{m}_{t2} = \left( \frac{2}{k+1} \right)^{\frac{1}{2} \left( \frac{k+1}{k-1} \right)} \cdot \sqrt{k} \cdot A_c \cdot \frac{p_m}{\sqrt{RT_m}} = 0.029 [kg/s] \quad (8)$$

The real mass flow for the 2<sup>nd</sup> version at  $\Delta p = 6 \cdot 10^2 [Pa]$  is:

$$\dot{m}_1 = \dot{m}_2 = \alpha_{2r} \dot{m}_{t1} = 0.8 \cdot 0.029 = 0.023 [kg/s] \quad (9)$$

### 3. CFD (Computational Fluid Dynamics) simulation of the flow through the restrictors of second stage regulator

For a comparative analysis of the theoretical results, we proceeded to the second method of studying the turbulent flow of respiratory gas through the studied pneumatic mechanisms: CFD (Computational Fluid Dynamics) simulation. Ansys Fluent is a general purpose numerical finite element modeling package that solves a wide range of mechanical computational problems. These problems include dynamic, structural analysis (both linear and nonlinear), heat and fluid transfer. [6]

CFD simulation is a modern method, that allows the calculation to be resumed on several models of nozzles and with changing flow conditions, so as to reach an ideal shape. In order to establish the favorable geometric conditions for reducing the external respiratory resistances of the breathing apparatus, we used all 5 parts of the program, respectively: Geometry, Meshing, Setting, Solution and Results. [7]

The program used results in a wider view of the variation of several physical sizes: pressure, density, velocity, mass flow.

We obtained the geometry of the fluid that goes through the two constructive variants and we made the meshing of these two models.

The imposed conditions have been set:

- turbulent and stationary flow (viscous);
- environment: fluid compressible air and its properties;
- variable density with pressure;
- the absolute inlet pressure imposed:  $9.5 \cdot 10^5 [Pa]$ ;
- the differential pressure imposed:  $\Delta p = 5 \cdot 10^2 [Pa]$ .

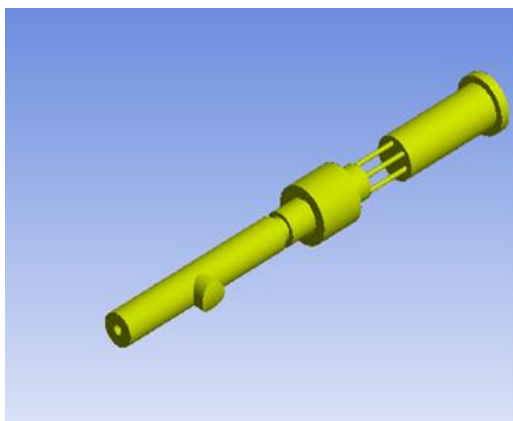


Fig. 3 The mass airflow rate for the 1<sup>st</sup> version [8]

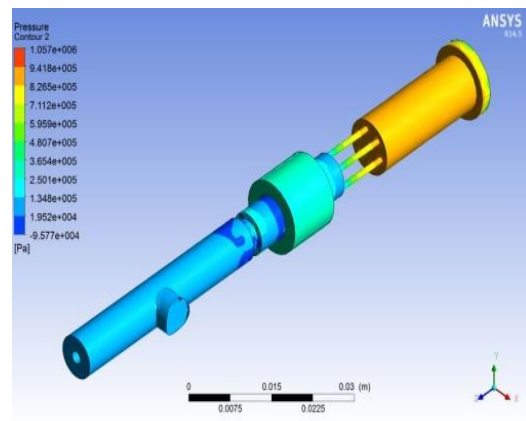
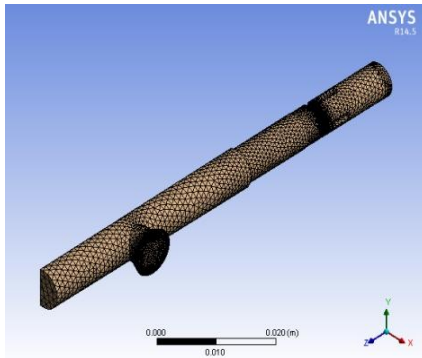
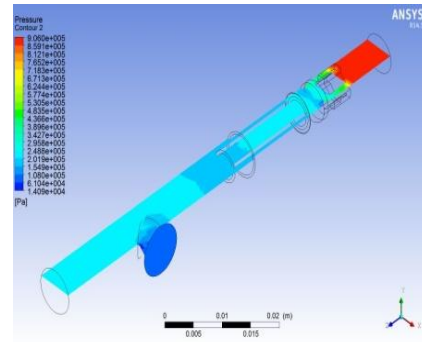


Fig. 5 Distribution of pressures in 1<sup>st</sup> version [8]



**Fig. 4 Meshing of the mass airflow rate for the 2<sup>nd</sup> version [8]**



**Fig. 6 Distribution of pressures in 2<sup>nd</sup> version [8]**

In both variants (cylindrical orifice and conical orifice), the sudden drop in pressure when passing through restriction A is very well observed, a fall which is specific to the Laval nozzle (see Figure 5 and Figure 6).

Ansys Fluent also allows the calculation of mass flows. The mass airflow is constant, for the same flow conditions at the same device. It depends on the opening of the restrictor A (in this case we set  $x = 0.7\text{mm}$  constant, for all the chosen constructive versions) and on the area of the fixed restrictor B. The mass airflows calculated with Ansys Fluent are:

$\dot{m}_1 = 15.225 \cdot 10^{-3} [\text{kg/s}]$  for *the 1<sup>st</sup> version*, with cylindrical area ( $d = 5 \cdot 10^{-3}\text{m}$ )  
 $\dot{m}_2 = 16.433 \cdot 10^{-3} [\text{kg/s}]$  for *the 2<sup>nd</sup> version*, with conical area ( $d = 6 \cdot 10^{-3}\text{m}$ ).

#### **4 . Experimental validation of the potential mass airflows through the two versions of diver's breathing apparatus**

The experimental verification was made at the Hyperbaric Laboratory of the Diving Center, for the two versions of the pressure regulator in Figures 7 and 8, at the professional Scuba Tools tester in Figure 9.



**Fig. 7 The 1<sup>st</sup> version piston with cylindrical orifice [8]**



**Fig. 8 The 2<sup>nd</sup> version piston with conical orifice [8]**



**Fig. 9 Second stage regulator testing [8]**



The supply of the tested devices was made from a bottle with  $150 \cdot 10^5 Pa$ , reduced to the average pressure in the hose measured  $p_m = 9.5 \cdot 10^5 Pa$ . The differential opening pressure was increasing  $(1 + 6) \cdot 10^2 Pa$ . It was measured on the differential manometer of the stand; we noted the volume airflow  $\dot{V}$ , recorded at the flow meter, corresponding to the differential pressures of  $5 \cdot 10^2 Pa$  and  $6 \cdot 10^2 Pa$  respectively. The mass airflow  $\dot{m}$  [kg/s] is:

$$\dot{m} = \rho \cdot \dot{V} \quad (10)$$

The values of the mass flows calculated on the basis of the measurements made are found in Table 1, chapter 5.

## 5. Results obtained and final conclusions

**Table 1 Numerical air flow values calculated numerically, by CFD simulation and experimentally verified**

Calculation method	Debit masic $\dot{m}$ [kg/s]			
	The 1 <sup>st</sup> version cylindrical orifice		The 2 <sup>nd</sup> version with conical orifice	
Numerical calculus	$\Delta p = 5 \cdot 10^2 Pa$	$\Delta p = 6 \cdot 10^2 Pa$	$\Delta p = 5 \cdot 10^2 Pa$	$\Delta p = 6 \cdot 10^2 Pa$
CFD Simulation	$17.5 \cdot 10^{-3}$	$20 \cdot 10^{-3}$	$20 \cdot 10^{-3}$	$23 \cdot 10^{-3}$
Experimental verification	$15,225 \cdot 10^{-3}$	$11.3 \cdot 10^{-3}$	$16,433 \cdot 10^{-3}$	$12.7 \cdot 10^{-3}$
	$10,2 \cdot 10^{-3}$		$11,9 \cdot 10^{-3}$	

It can be concluded:

- The theoretical values for the air flow were calculated for ideal gas, for a simplified model in which we took into consideration only two serial pressure restrictors: **A** and **B**.
- The surface of the first limiter is variable in time, but the smallest cross section of the airflow remains, thus fulfilling the conditions for a critical flow.
- The flow is stationary for the same environmental parameters and consequently the air mass flow depends only on the x opening of the **A** restrictor, caused by the differential pressure  $\Delta p$ .
- After the thin wall flow coefficients ( $\alpha_1 = 0.7$  and  $\alpha_2 = 0.8$ ) were applied to the mass flows, the highest values remain those obtained by the theoretical calculation.
- The conical section of the **B** restrictor determined a slightly higher flow rate in all three methods (theoretical calculation, numerical simulation and experimental verification).
- The performance techniques used in the numerical simulation make it possible to refine the calculations and to highlight the influence of the constructive form of the respiratory gas circuit restrictors through the apparatus.

Breathing gas flow modeling by the pressure regulators mechanisms of diver's apparatus, with CFD - ANSYS Fluent, has been shown to be useful in the ergonomic study of the design of devices used by divers. The simulation can also be resumed under operating conditions at required immersion depths (various outlet pressures).

The knowledge of the respiratory flow of gas in various situations, through the geometric study of the constructive versions, completes the possibility of controlling the physical and physiological phenomena involved.

The theoretical and experimental results obtained can be the basis for the elaboration of a program for periodic verification and adjustment of the pressure regulators in the divers' equipment.

## References

- [1] Stanciu T., Constantin A., 2018, *Theoretical and experimental study of turbulent gas flow through a pneumatic mechanism*, 18th International Multidisciplinary Scientific GeoConference SGEM Marine and Ocean Ecosystems, Albena, Bulgaria, vol. 18, pag. 1205-1212
- [2] Carafoli E., Constantinescu M., 1984, *Dynamics of compressible fluids*, Publishing house of the Romanian Academy, Bucharest.
- [3] Petcu D., *Pneumoautomatica*, 1970, Technical Ed., Bucharest.
- [4] Dinu D, 2013, *Fluid Mechanics for navigators*, pg. 39, Nautica, Constantza.
- [5] Constantin A. , 2003, *Gas Transport through the underwater breathing apparatuses*, Ovidius University Press, Constanta.
- [6] Niță C.M., Scurtu IC, Cupsa O, 2018, *Review in Numerical Simulation in Naval Application*, Journal of Physics Conference Series, 1122(1), art. no. 012020.
- [7] Scupi A, Dinu D, , 2015, *Fluid Mechanics Numerical Approach*, Nautica Ed., Constantza.
- [8] Stanciu T., 2018, *Research on gas transfer in diving technologies*, Ph.D. Thesis, Maritime University Constantza.